JOURNAL OF VIROLOGY, Nov. 2006, p. 11385–11392 Vol. 80, No. 22
0022-538X/06/$08.00+0 doi:10.1128/JVI.00439-06

African Swine Fever Virus Causes Microtubule-Dependent Dispersal of the *trans*-Golgi Network and Slows Delivery of Membrane Protein to the Plasma Membrane▽

Christopher L. Netherton,[1]* Mari-Clare McCrossan,[1]¶ Michael Denyer,[1] Sreenivasan Ponnambalam,[2] John Armstrong,[3] Haru-Hisa Takamatsu,[1] and Thomas E. Wileman[1]‡

Department of Immunology, Pirbright Laboratory, Institute for Animal Health, Ash Road, Woking GU24 0NF,[1] Faculty of Biological Sciences, University of Leeds, Leeds LS2 9JT,[2] and Department of Biochemistry, School of Life Sciences, University of Sussex, Falmer BN1 9QG,[3] United Kingdom

Received 2 March 2006/Accepted 28 August 2006

Viral interference with secretory cargo is a common mechanism for pathogen immune evasion. Selective down regulation of critical immune system molecules such as major histocompatibility complex (MHC) proteins enables pathogens to mask themselves from their host. African swine fever virus (ASFV) disrupts the *trans*-Golgi network (TGN) by altering the localization of TGN46, an organelle marker for the distal secretory pathway. Reorganization of membrane transport components may provide a mechanism whereby ASFV can disrupt the correct secretion and/or cell surface expression of host proteins. In the study reported here, we used the tsO45 temperature-sensitive mutant of the G protein of vesicular stomatitis virus to show that ASFV significantly reduces the rate at which the protein is delivered to the plasma membrane. This is linked to a general reorganization of the secretory pathway during infection and a specific, microtubule-dependent disruption of structural components of the TGN. Golgin p230 and TGN46 are separated into distinct vesicles, whereupon TGN46 is depleted. These data suggest that disruption of the TGN by ASFV can slow membrane traffic during viral infection. This may be functionally important because infection of macrophages with virulent isolates of ASFV increased the expression of MHC class I genes, but there was no parallel increase in MHC class I molecule delivery to the plasma membrane.

Many DNA viruses encode proteins that interfere with the transport of immunologically important molecules within the secretory pathway. This is thought to allow viruses to evade host immune responses and may also contribute to the pathology and progression of disease. Members of the herpesvirus family encode proteins that interfere with the assembly and presentation of major histocompatibility complex (MHC) class I peptide complexes (2, 11). Similarly, the adenovirus E13/19K glycoprotein binds and retains MHC class I molecules in the endoplasmic reticulum (ER) (6), while cytomegaloviruses also down regulate the cell surface expression of MHC class II molecules in professional antigen-presenting cells (26). On the other hand, DNA viruses also make active use of the secretory pathway to secrete homologues of cellular signaling molecules and their receptors that act as decoy proteins to suppress immune responses. Poxviruses, for example, encode homologues of the tumor necrosis factor and gamma interferon receptors and interleukin-10 (IL-10), as well as a granulocyte-macrophage colony-stimulating factor binding protein (1). Herpesviruses encode a number of cytokine and chemokine homologues, including IL-6 and IL-10 (1).

African swine fever virus (ASFV) is a large double-stranded DNA virus that replicates primarily in cells of the mononuclear phagocyte system of swine. Unlike the other DNA viruses, ASFV appears to lack a large complement of immunoregulatory proteins that are targeted to the secretory pathway to subvert specific components of the host immune response (40). The principal exception to this is the product of the EP402R gene, which is a viral homologue of CD2 and, in conjunction with the product of the EP135R gene, recruits erythrocytes to infected cells. This may sterically mask virally infected cells from cytotoxic white blood cells (5, 12, 33). ASFV also encodes an inhibitor of nuclear factor κB (NF-κB) and nuclear factor of activated T cells, which can repress proinflammatory immune responses (25, 29, 36). Interestingly, ASFV may alter host responses to the virus by targeting the secretory pathway itself, rather than specific immunomodulatory proteins secreted by cells. Our previous work (23) has shown that ASFV causes disruption of the *trans*-Golgi network (TGN), and this is characterized by the loss of TGN46, an integral membrane protein involved in maintaining the morphology of the TGN (4), and AP1, an adaptor protein important for the correct sorting of secretory cargo leaving the TGN. If disruption of the TGN causes slowing or cessation of protein trafficking to the cell surface, this could be a major benefit in immune evasion by selective targeting of MHC class I molecules, as well as significantly altering the host's immune response by reducing secretion by macrophages, which are ASFV's principal target of infection.

* Corresponding author. Mailing address: Pirbright Laboratory, Institute for Animal Health, Ash Road, Pirbright, Surrey GU24 0NF, United Kingdom. Phone: 44 1483 232441. Fax: 44 1483 232448. E-mail: chris.netherton@bbsrc.ac.uk.

¶ Present address: Laboratory for Clinical and Molecular Virology, University of Edinburgh, Summerhall, Edinburgh, Scotland EH9 1QH, United Kingdom.

‡ Present address: Infection and Immunity, School of Medicine, Health Policy and Practice, Institute of Health, University of East Anglia, Norwich NR4 TJU, United Kingdom.

▽ Published ahead of print on 6 September 2006.

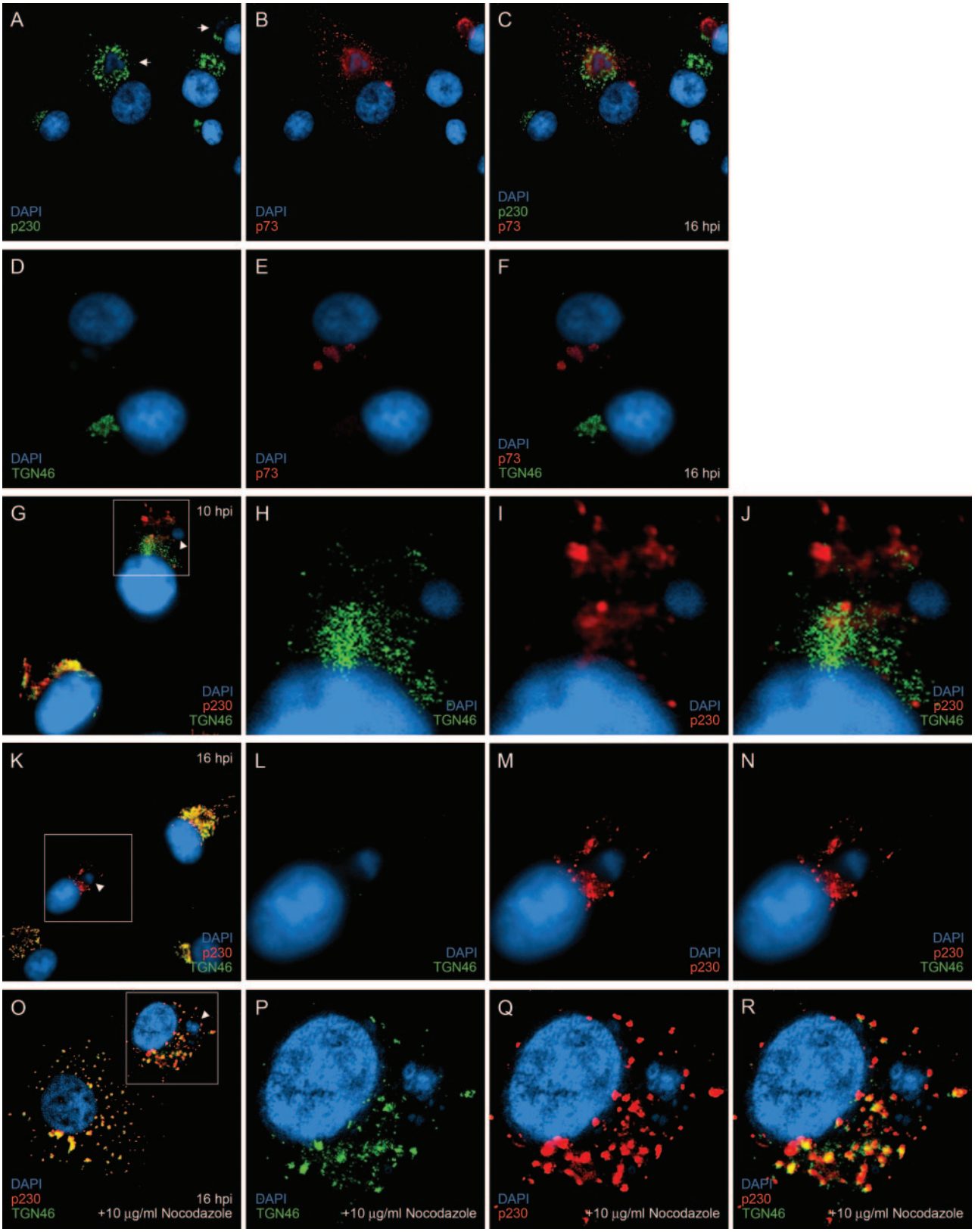

FIG. 1. The effect of ASFV on TGN is microtubule dependent. Vero cells grown on coverslips were infected for 16 h with the Vero cell-adapted Badajoz 1971 (Ba71v) strain of ASFV (A to N) or infected for 8 h with Ba71v and incubated for a further 8 h in the presence of 10 μg/ml nocodazole (O to R) and then fixed, permeabilized, and processed for indirect immunofluorescence. The cells were stained with p230 antiserum (A) or sheep anti-TGN46 (D, G, K, and O) and 4H3 (B and E) or p230 antiserum (G, K, and O) and then with appropriate secondary antibodies conjugated to Alexa-488 or -594. All cells were incubated with DAPI (4′,6′-diamidino-2-phenylindole) dye. The cells were viewed at 60× magnification (1.4

To further characterize the effect of ASFV infection on the TGN, we followed the distribution of golgin p230, a peripheral protein that localizes to the organelle. Figure 1A to C show that p230 was redistributed from the compact juxtanuclear Golgi pattern seen in uninfected cells to a punctate stain concentrated around the viral factory in infected cells. In a similar experiment, the results for infected cells labeled with anti-TGN46 (Fig. 1D to F) confirmed that infection with ASFV led to the loss of the immunofluorescence staining pattern for TGN46. We have shown previously that TGN46 first starts to disappear approximately 10 h postinfection (hpi) (23), and we were therefore interested to determine the effect of ASFV on the two markers relative to each other as infection progressed. At 10 hpi, both markers were present in infected cells (Fig. 1G to J), but in contrast to uninfected cells, TGN46 and p230 were not colocalized and had separated into two distinct staining patterns that showed minimal overlap (Fig. 1J). At 16 hpi, the TGN46 signal had completely disappeared from the infected cell (Fig. 1K and L), whereas the p230 signal remained (Fig. 1M) and in most of the cases examined was clustered around the virus factory. This showed that in uninfected cells, p230 and TGN46 colocalize but that during ASFV infection, the two proteins become separated into what appear to be distinct vesicular populations. The signal for TGN46 is then lost, while p230 is not and remains in the vicinity of the virus factory.

Since sites of ASFV replication lie close to the microtubule-organizing center (15, 18) and the microtubule network plays a major role in the correct localization and maintenance of the Golgi apparatus and TGN (8, 41), the effect of nocodazole on the redistribution of TGN markers during ASFV infection was tested. Vero cells were infected for 8 h with the tissue culture-adapted Badajoz 1971 (Ba71v) strain of ASFV (9) to allow initiation of DNA and late protein synthesis and then incubated for a further 8 h with nocodazole to depolymerize the microtubules. Figure 1O to R demonstrate that depolymerization of the microtubules led to the redistribution of TGN46 and p230 from a juxtanuclear localization to a punctate stain dispersed throughout the cytosol (compare the lower cell in Fig. 1O to the uninfected cells in Fig. 1G and K). Most striking was the observation that nocodazole prevented the ASFV-induced loss of the TGN46 signal and that TGN46 and p230 remained colocalized in the infected cell. The results suggested that the separation of these two TGN markers and the subsequent loss of the TGN46 staining pattern were microtubule dependent.

In order to determine whether the redistribution of TGN proteins had a specific effect on the TGN or was a part of a large-scale reorganization of the secretory pathway during ASFV infection, the integrity of other compartments of the secretory pathway was studied. Antibodies were used to localize the ER, the ER-Golgi intermediate compartment (ERGIC), the central Golgi stacks, and the *trans*-Golgi cisternae. Infected cells were identified using an antibody specific for p73, the major capsid protein of ASFV (7), or antibodies raised against pE183L, a viral protein located in factories (35). Figure 2A to C show an apparent lack of the ER marker calnexin in the perinuclear regions of the infected cells that colocalized with p73, suggesting that calnexin was excluded from ASFV viral factories. Similar results have been described for the ER lumenal protein disulfide isomerase (28) and the ER membrane protein p63 (3). The ERGIC marker protein ERGIC-53 was dispersed and excluded from areas of viral replication but appeared as a compact juxtanuclear crescent in uninfected cells (Fig. 2D to F). Similarly, the resident Golgi protein GM130 was in a compact perinuclear crescent, typical of a resident Golgi marker in uninfected cells, but was also dispersed in infected cells positive for p73 (Fig. 2G to I). Cells where the *trans*-cisternae of the Golgi apparatus were labeled with GalNAc-T2-green fluorescent protein (GFP) are shown in Fig. 2J to L. Again, there was compact perinuclear staining in cells negative for p73, but the GalNAc-T2-GFP signal was dispersed in infected cells. Taken together, the results showed that membrane compartments proximal to the TGN are disrupted in cells infected by ASFV, but unlike the TGN, they are not lost from the cell.

ASFV infection inhibits the processing of cathepsin D into its mature form, a process that is dependent on the transport of the protein from the ER through the Golgi apparatus to lysosomes (23, 32), which suggests that the virus may also reduce the rate of secretion to the cell surface. To directly determine the effect of ASFV infection on the transport of secretory cargo to the plasma membrane, we utilized the temperature-sensitive glycoprotein from the tsO45 mutant of vesicular stomatitis virus (VSV-GtsO45) (10). Fusions between VSV-GtsO45 and fluorescent proteins have been used extensively to characterize the secretory pathway (16, 24, 31) and were recently used to assess the effect of viral infection thereon (27). At the nonpermissive temperature of 40°C, the F204S mutation prevents ER exit, but at the permissive temperature of 32°C, VSV-GtsO45 folds correctly and exits the ER (13, 19). Vero cells expressing VSV-GtsO45-yellow fluorescent protein (27) were infected overnight with Ba71v at 40°C to accumulate the protein in the ER. Half the cells were then shifted to 32°C to allow transport of VSV-G through the secretory pathway. The cells were left for 3 h, at which point the majority of VSV-G should have reached the plasma membrane in the cells that had been shifted to 32°C (16). Finally, the cells were fixed and stained with an antibody recognizing an ASFV multigene family protein, pY118L (28), to identify viral infection and I1 to enhance detection of cell surface VSV-G protein (20). Inspection of representative images of cells after incubation at 40°C or 32°C (Fig. 3A) revealed that at the nonpermissive temperature (40°C), VSV-G protein was retained in the ER, while at 32°C, the majority of the protein appeared at the cell surface. However, some of the cells incubated at 32°C did not display a characteristic plasma membrane localization for

normal aperture) with a Nikon E800 microscope. Images were captured with a Hamamatsu C-4746A charge-coupled-device camera and were deconvolved and digitally merged with Improvision Openlab 2.1.3 software. Twenty optical sections 0.2 μm thick were analyzed. The images were resized and annotated using Adobe Photoshop CS 8. Arrows indicate recruitment of p230 to viral factories, arrowheads indicate viral factories, and boxed areas designate the region enhanced in the subsequent three panels.

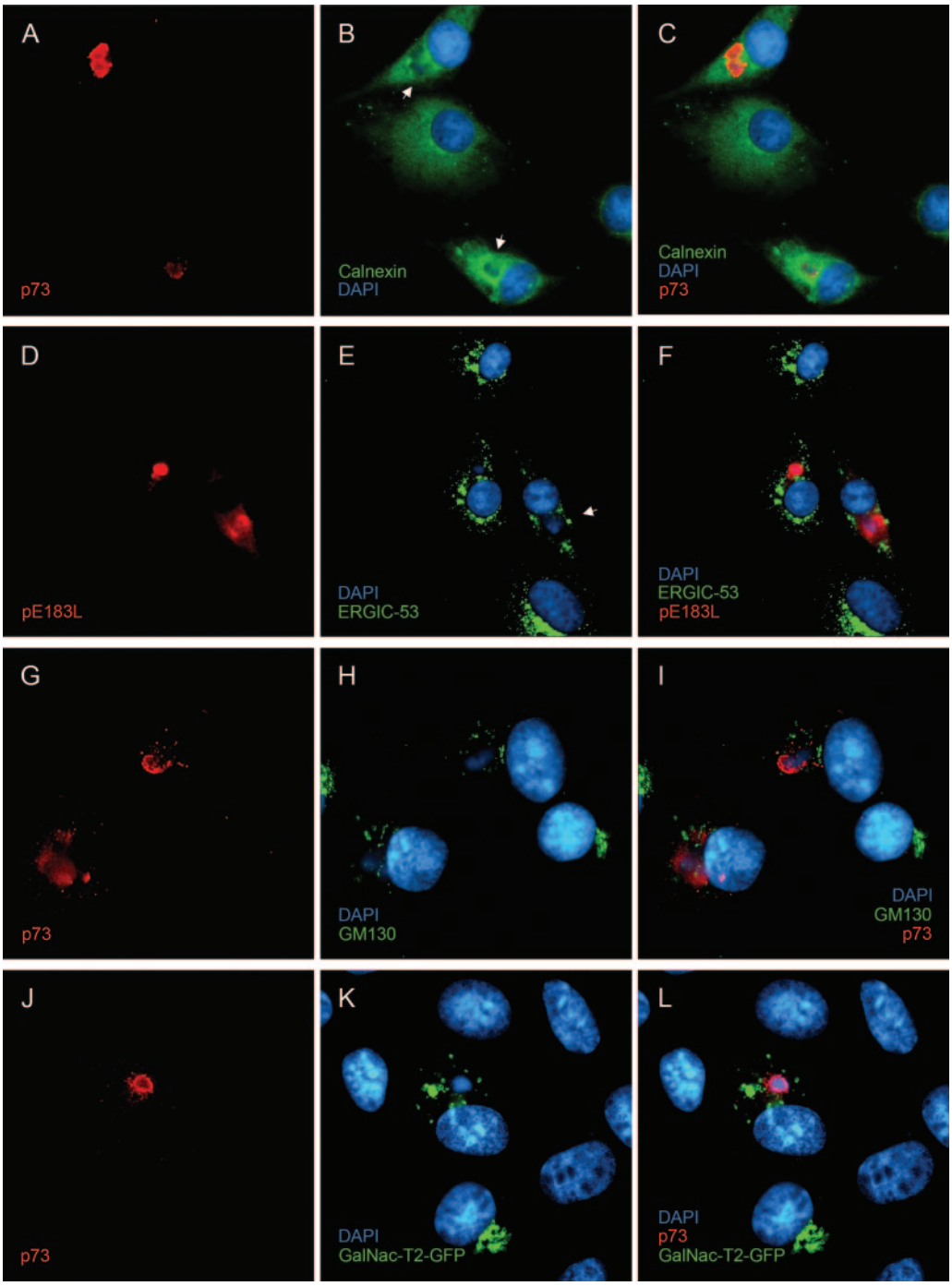

FIG. 2. Effect of ASFV on markers of the secretory pathway. Vero cells grown on coverslips were infected for 16 h with Ba71v and then fixed, permeabilized, and processed for indirect immunofluorescence. The cells were stained with 4H3 (A, G, and J) or RB7 (D) and calnexin (B), G1/93 (E), or GM130 (H) antiserum and then with appropriate secondary antibodies conjugated to Alexa-488 or -594. All cells were incubated with DAPI dye (B, E, H, and K). The cells were viewed at 60× magnification (1.4 normal aperture) with a Nikon E800 microscope. Images were captured with a Hamamatsu C-4746A charge-coupled-device camera and were deconvolved and digitally merged using Improvision Openlab 2.1.3 software. Twenty optical sections 0.2 μm thick were analyzed. Images were resized and annotated using Adobe Photoshop CS 8. Arrows indicate the positions of virus replication sites.

VSV-G; in such cells, VSV-G was present in small dispersed vesicles within the cytoplasm. Colabeling with an antibody to the early ASFV protein pY118L revealed that the cells lacking VSV-G plasma membrane staining expressed viral pY118L. This suggests that ASFV infection blocks or slows the transport of VSV-G to the cell surface.

Microscopy of infected cells was analyzed in a quantitative manner: 2,343 cells were examined, and the subcellular local-

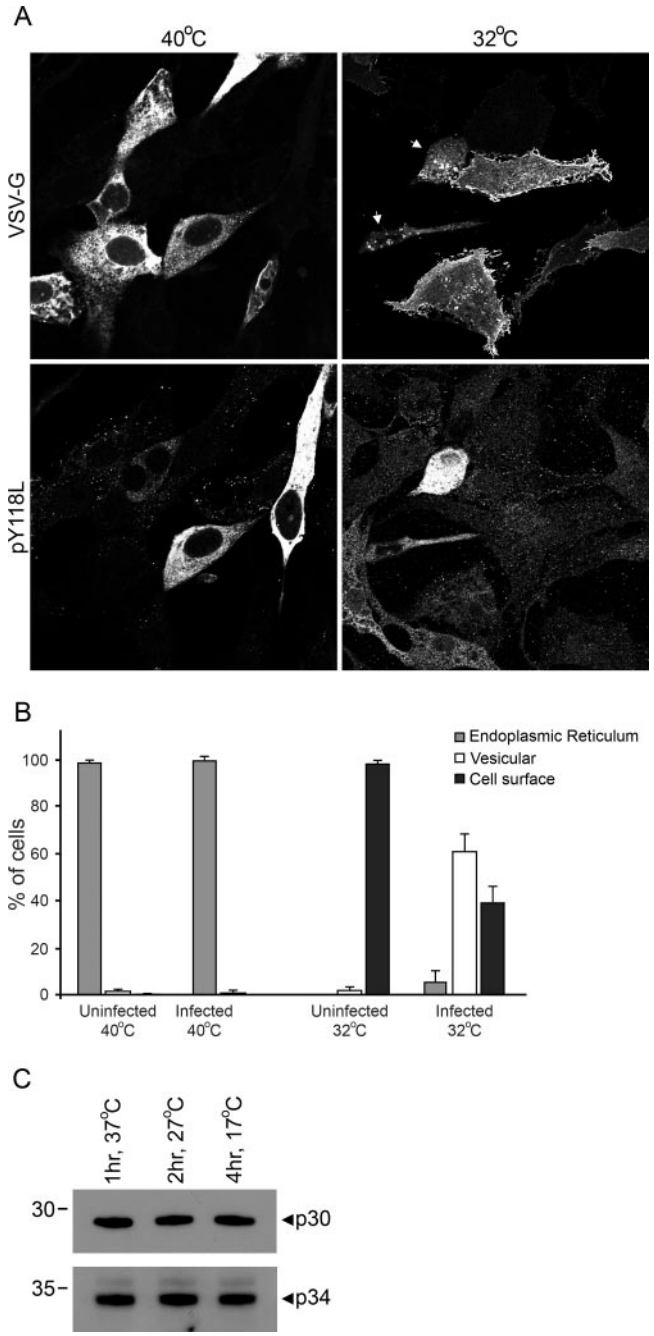

FIG. 3. ASFV retards the transport of VSV-G to the cell surface. (A and B) Vero cells were transfected with pVSVΔK-YFP and then infected with Ba71v 24 h later. After the inoculum was washed off, the cells were transferred to 40°C and left overnight. The following day, the cells were shifted to 32°C or 40°C and incubated for a further 3 h prior to being fixed and permeabilized. The cells were stained with R30 and I1 to stain pY118L and VSV-G, respectively, and then with appropriate secondary antibodies conjugated to Alexa-488 or -594. (A) Cells were viewed at 60× magnification (1.4 normal aperture) with a Nikon E800 microscope. Images were captured with a Hamamatsu C-4746A charge-coupled-device camera and were deconvolved using Improvision Openlab 3.1.7 software. Ten optical sections 0.2 μm thick were analyzed. Arrows indicate infected cells expressing VSV-G. (B) Graphical representation of cell count experiments (eight experiments for each temperature) comparing the natures of VSV-G subcellular localization in uninfected and infected cells after 3 h of incubation at 32°C or 40°C. (C) Vero cells were infected for 12 h with Ba71v at 37°C and then incubated for either one further hour at 37°C, 2 h at 27°C, or 4 h at 17°C. The cell lysates were subjected to SDS-polyacrylamide gel electrophoresis and then immunoblotted with anti-p30 monoclonal C18 or anti-p34 antiserum TW34. The positions of molecular mass markers are indicated to the left of each gel. The images and gel scans were resized and annotated using Adobe Photoshop CS 8.

ization of VSV-G was recorded as being either in the ER (reticular staining emanating from the nuclear envelope to the periphery), vesicular (nonreticular staining with an absence of cell surface labeling), or at the cell surface (any cell surface labeling, irrespective of intracellular signal). The percentage of VSV-G-positive cells having ER, vesicular, or surface labeling was calculated for both infected and uninfected cells, and a mean percentage was derived for each localization at both 32°C and 40°C in the presence or absence of virus. The differences between the percentages of infected and uninfected cells expressing VSV-G in a particular subcellular compartment at a given temperature were analyzed with a paired t test with 95.0% confidence levels using Minitab 13.32. There was little difference in nature between the VSV-G staining of uninfected cells and that of infected cells that had been incubated at 40°C; 98.3% of uninfected VSV-G-expressing cells and 99.2% of infected VSV-G-expressing cells had ER staining ($t = -1.26$, $P = 0.249$), 1.5% and 0.8% had vesicular labeling ($t = -1.15$, $P = 0.290$), and 0.2% and 0% had cell surface staining ($t = -1.00$, $P = 0.351$) (Fig. 3B). After the temperature was shifted to 32°C for 3 h, significant differences between the patterns of VSV-G staining of uninfected and infected cells became apparent. Figure 3B shows that the number of cells with surface expression of the VSV-G protein fell from 97.8% to 38.9% following infection with ASFV ($t = 21.29$, $P = \leq 0.001$), and this correlated with increased intracellular staining for the VSV-G protein, the bulk of which was vesicular, rising from the 2.12% seen in uninfected cells to 55.8% when cells were positive for ASFV. Factoring in the 5.3% of infected cells that maintained ER staining showed that after 3 h at 32°C, 60.1% of infected cells showed intracellular VSV-G staining, compared to 2.12% of uninfected cells ($t = -21.29$, $P \leq 0.001$). ASFV infection therefore retards the transport of VSV-G to the cell surface at the permissive temperature.

It was important to ensure that the temperature shift had no adverse effects on viral replication, especially as lowered temperatures can block specific steps in the secretory pathway (34, 37). Pyrexia is concurrent with viremia during ASFV infection (38), so an inhibitory effect on viral replication from elevating the temperature to 40°C while preventing VSV-G exit from the ER was not anticipated. The Arrhenius equation predicts that rates of biological reactions will halve for each 10°C fall in temperature. To test if there was a specific block in viral replication at a lowered temperature, Vero cells were infected for 12 h and then incubated for a time that would compensate for the temperature change. Levels of viral proteins were then analyzed by immunoblotting of cell lysates with antibodies against the early ASFV protein p30 (30) and late structural protein p34 (15). Figure 3C shows that the rates of synthesis of both early and late viral proteins were not affected by temper-

ature decreases more than is predicted by simple reaction chemistry. This shows that there was no specific temperature block in ASFV replication.

Our studies described above showing slowed protein trafficking to the cell surface with a tissue culture-adapted isolate of ASFV led us to predict that infection of macrophages with virulent strains of the virus would down regulate the surface expression of immune response proteins. To test this, primary short-term monocyte/macrophage cell lines derived from peripheral blood monocytes of *cc* and *dd* inbred pigs were cultured for several weeks with recombinant porcine granulocyte-macrophage colony-stimulating factor (17) and the phenotype was confirmed by fluorescence-activated cell sorter analysis with CD172a antibody (data not shown); then these cells were infected with the Malawi Lil/20 isolate of ASFV overnight (14). The surface and total expression of MHC class I molecules was examined using antibody 2.27.3 (22), and the level of infection was assessed using antibody C18. Fluorescence-activated cell sorter (FACSCalibur; BD) analysis revealed that 89.94% of the *cc* cells and 76.13% of the *dd* cells expressed p30, indicating a high level of viral infection (data not shown). The geometric mean fluorescent intensity (MFI) of the total expression (surface and internal) of MHC class I molecules showed that ASFV infection up regulated class I molecule expression. This increase was moderate (15%) in *cc* cells, while in *dd* cells the total amount of MHC class I molecules nearly trebled (Fig. 4A). Importantly, the increase in the total amount of MHC class I molecules did not lead to a proportionate increase in the delivery of MHC class I molecules to the plasma membrane. In both cell types, ASFV caused the surface pool of MHC class I molecules to decrease as a percentage of the total amount of MHC class I molecules (Fig. 4B). For *cc* pigs, the percentage of MHC class I molecules on the cell surface was halved (38% to 18%) by ASFV infection. The effect was less dramatic for *dd* pigs, but the threefold increase in MHC class I gene expression caused by infection with ASFV resulted in only a twofold increase in the surface pool of MHC class I molecules. The reasons for the difference between *cc* and *dd* cells are not known, but these were single-time-point experiments chosen to correlate with the trafficking experiments performed with the VSV-G protein in Vero cells, where the effects of ASFV were monitored soon after the induction of late gene expression. It is possible that a greater effect on MHC class I genes may be apparent if the experiments with macrophages are repeated at later time points. Importantly, the results do show that the trafficking of an immunologically important protein to the cell surface is slowed by a virulent strain of ASFV in primary cells relevant to the speed of infection by ASFV in vivo and that this correlates with the effects of ASFV on VSV-G protein transport in a standard protein-trafficking assay.

In summary, these data extend our previous observation and show that disruption of the TGN by ASFV involves an initial dispersion of the organelle and separation of the integral membrane protein TGN46 from the peripheral TGN golgin p230. Interestingly, during this initial phase, the signals for TGN46 and p230 remain vesicular, suggesting separation of the TGN into two biochemically distinct membrane populations. Both these vesicles migrate towards the viral factories but whereas the p230-containing vesicles persist during infection, the TGN46-positive vesicles are subsequently lost (Fig. 1A to N).

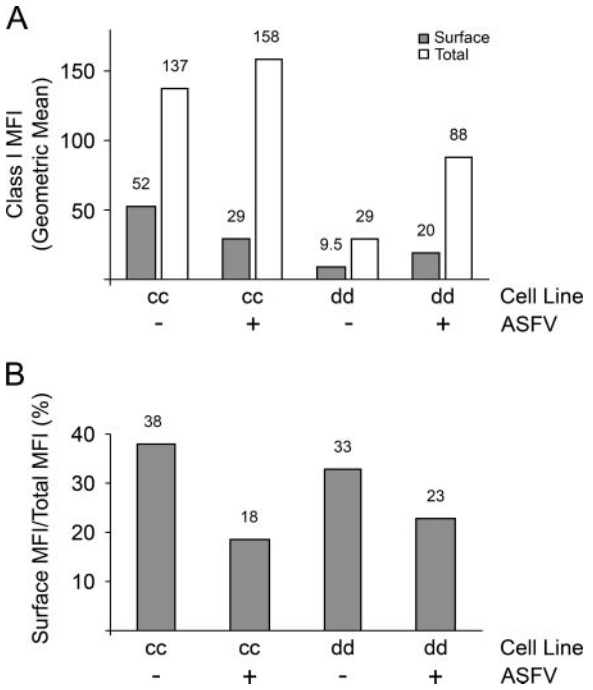

FIG. 4. ASFV down regulates MHC class I molecule surface expression. (A) Monocyte/macrophage cultures from *cc* and *dd* inbred pigs were mock infected or infected with ASFV overnight. The cells were stained with 2.27.3 monoclonal antibody and then anti-immunoglobulin G2a conjugated to R-phycoerythrin. Half of the cells were permeabilized and restained with 2.27.3. The cells were then subjected to FACSCalibur analysis, and the MFIs of surface and total amounts MHC class I molecules were calculated. (B) Data from panel A showing the surface MFI expressed as a percentage of the total MFI. The numbers above the columns show the values of the data points. In separate experiments, the MFIs of internal MHC class I molecule staining were confirmed by using different fluorophores for internal and surface staining with and without a block of unconjugated isotype-specific antibody between the internal and surface stainings. Internal staining was also performed in the absence of surface staining. In all cases, the controls supported the observation that ASFV infection up regulates total MHC class I molecule expression yet suppresses the surface expression of the protein (data not shown).

Viral factories are located next to the microtubule-organizing center, suggesting that microtubules may be involved in the dispersal and movement of these TGN proteins. This is supported by the observation that the dispersal of TGN46 and golgin p230 into separate vesicles was inhibited when the microtubules were depolymerized by nocodazole, as was the loss of the TGN signal (Fig. 1O to R). We also examined the functional consequences of TGN loss and show that infection with ASFV reduces the delivery of a model type 1 membrane protein, the G protein of VSV, to the plasma membrane. This is consistent with the accepted role of the tubulovesicular TGN as an organelle that controls the sorting and anterograde movement of proteins after their arrival from the cisternal *trans* subcompartment of the Golgi apparatus. Similar but distinct effects on the TGN have been observed during herpes simplex virus infection and cholesterol loading (39, 42). Both of these conditions induce the redistribution of TGN elements, but in contrast to ASFV infection, the integrity of the organelle is unaffected because the TGN markers are not lost and re-

main colocalized. Another critical difference is that cholesterol-induced movement of TGN proteins is not dependent on microtubules; rather, it involves actin filaments (42).

Disruption of vesicular transport at the TGN provides ASFV with a mechanism to slow the arrival of important immune surveillance factors to the plasma membrane, and we have demonstrated this in principal for the delivery of MHC class I molecules to the cell surfaces of macrophages infected with virulent ASFV. It is important to note that we do not have direct evidence that the slowed delivery of MHC class I molecules to the cell surface compromises the recognition of infected cells by cytotoxic T lymphocytes. We do know, however, that even though ASFV infection increases the expression of MHC class I genes in *cc* and *dd* cell lines, the bulk of the MHC class I molecules induced by ASFV infection remains intracellular. This may be important in the context of infection, as the newly synthesized MHC molecules induced by ASFV would likely be loaded with viral rather than self-peptides. Therefore, slowing the surface expression of MHC molecules loaded with viral peptides may reduce cytotoxic-T-lymphocyte-mediated host cell lysis early enough to allow a productive infection, while avoiding NK cell-mediated cell lysis that may be induced by a total block in secretion. Further experiments will be required to determine whether ASFV infection affects the turnover of MHC class I molecules on the cell surface and whether this leads to the increased NK activity observed during ASFV infection (21) or to a reduced ability to present antigens to T cells. ASFV is a macrophage-tropic virus, and inhibition of anterograde transport may significantly alter the immune response of infected animals in other ways where functional disruption of the secretory pathway would be predicted to affect the secretion of many crucial cytokines and chemokines. Efforts are under way to determine if this occurs in vivo.

We thank Marvin J. Fritzler (University of Calgary, Canada) for the antibodies to GM130 and p230, Neil J. Bulleid (University of Manchester) for the antibody against calnexin, Hans-Peter Hauri (University of Basel, Switzerland) for anti-ERGIC53 antibody, Doug Lyle for monoclonal I1, and Jamie White (Heidelberg, Germany) for the pEGFP-N1-GalNAc-T2 plasmid.

REFERENCES

1. **Alcami, A.** 2003. Viral mimicry of cytokines, chemokines and their receptors. Nat. Rev. Immunol. **3:**36–50.
2. **Ambagala, A. P. N., J. C. Solheim, and S. Srikumaran.** 2005. Viral interference with MHC class I antigen presentation pathway: the battle continues. Vet. Immunol. Immunopathol. **107:**1–15.
3. **Andrés, G., R. García-Escudero, C. Simón-Mateo, and E. Viñuela.** 1998. African swine fever virus is enveloped by a two-membraned collapsed cisterna derived from the endoplasmic reticulum. J. Virol. **72:**8988–9001.
4. **Banting, G., and S. Ponnambalam.** 1997. TGN38 and its orthologues: roles in post-TGN vesicle formation and maintenance of TGN morphology. Biochim. Biophys. Acta **1355:**209–217.
5. **Borca, M. V., C. Carrillo, L. Zsak, W. W. Laegreid, G. F. Kutish, J. G. Neilan, T. G. Burrage, and D. L. Rock.** 1998. Deletion of a CD2-like gene, 8-DR, from African swine fever virus affects viral infection in domestic swine. J. Virol. **72:**2881–2889.
6. **Burgert, H. G., and S. Kvist.** 1985. An adenovirus type 2 glycoprotein blocks cell surface expression of human histocompatibility class I antigens. Cell **41:**987–997.
7. **Cobbold, C., J. T. Whittle, and T. Wileman.** 1996. Involvement of the endoplasmic reticulum in the assembly and envelopment of African swine fever virus. J. Virol. **70:**8382–8390.
8. **Cole, N. B., N. Sciaky, A. Marotta, J. Song, and J. Lippincott-Schwartz.** 1996. Golgi dispersal during microtubule disruption: regeneration of Golgi stacks at peripheral endoplasmic reticulum exit sites. Mol. Biol. Cell **7:**631–650.
9. **Enjuanes, L., A. L. Carrascosa, M. A. Moreno, and E. Viñuela.** 1976. Titration of African swine fever (ASF) virus. J. Gen. Virol. **32:**471–477.
10. **Flamand, A.** 1970. Etude génétique du virus de la stomatite vésiculaire: classement de mutants thermosensibles spontanés en groupes de complémentation. J. Gen. Virol. **8:**187–195.
11. **Früh, K., A. Gruhler, R. M. Krishna, and G. J. Schoenhals.** 1999. A comparison of viral immune escape strategies targeting the MHC class I assembly pathway. Immunol. Rev. **168:**157–166.
12. **Galindo, I., F. Almazán, M. J. Bustos, E. Viñuela, and A. L. Carrascosa.** 2000. African swine fever virus EP135R open reading frame encodes a glycoprotein involved in the hemadsorption of infected cells. Virology **266:**340–351.
13. **Gallione, C. J., and J. K. Rose.** 1985. A single amino acid substitution in a hydrophobic domain causes temperature-sensitive cell-surface transport of a mutant viral glycoprotein. J. Virol. **54:**374–382.
14. **Haresnape, J. M., P. J. Wilkinson, and P. S. Mellor.** 1988. Isolation of African swine fever virus from ticks of the Ornithodoros moubata complex (Ixodoidae: Argasidae) collected within the African swine fever enzootic area of Malawi. Epidemiol. Infect. **101:**173–185.
15. **Heath, C. M., M. Windsor, and T. Wileman.** 2001. Aggresomes resemble sites specialized for virus assembly. J. Cell Biol. **153:**449–456.
16. **Hirschberg, K., C. M. Miller, J. Ellenberg, J. F. Presley, E. D. Siggia, R. D. Phair, and J. Lippincott-Schwartz.** 1998. Kinetic analysis of secretory protein traffic and characterization of Golgi to plasma membrane transport intermediates in living cells. J. Cell Biol. **143:**1485–1503.
17. **Inumaru, S., T. Kokuho, S. Denham, M. S. Denyer, E. Momotani, S. Kitamura, A. Corteyn, S. Brookes, R. M. E. Parkhouse, and H. Takamatsu.** 1998. Expression of biologically active recombinant porcine GM-CSF by baculovirus gene expression system. Immunol. Cell Biol. **76:**195–201.
18. **Jouvenet, N., and T. Wileman.** 2005. African swine fever virus infection disrupts centrosome assembly and function. J. Gen. Virol. **86:**589–594.
19. **Kreis, T. E., and H. F. Lodish.** 1986. Oligomerization is essential for transport of vesicular stomatitis viral glycoprotein to the cell surface. Cell **46:**929–937.
20. **Lefrancois, L., and D. S. Lyles.** 1982. The interaction of antibody with the major surface glycoprotein of vesicular stomatitis virus. Virology **121:**157–167.
21. **Leitão, A., C. Cartaxeiro, R. Coelho, B. Cruz, R. M. E. Parkhouse, F. C. Portugal, J. D. Vigário, and C. L. V. Martins.** 2001. The non-haemadsorbing African swine fever virus isolate ASFV/NH/P68 provides a model for defining the protective anti-virus immune response. J. Gen. Virol. **82:**513–523.
22. **Lunney, J. K., and M. D. Pescovitz.** 1988. Differentiation antigens of swine lymphoid tissue, p. 421–454. *In* M. Miyasaka and Z. Trnka (ed.), Differentiation antigens in lymphohemopoietic tissues. Marcel Dekker Inc., New York, N.Y.
23. **McCrossan, M., M. Windsor, S. Ponnambalam, J. Armstrong, and T. Wileman.** 2001. The *trans* Golgi network is lost from cells infected with African swine fever virus. J. Virol. **75:**11755–11765.
24. **Mezzacasa, A., and A. Helenius.** 2002. The transitional ER defines a boundary for quality control in the secretion of tsO45 VSV glycoprotein. Traffic **3:**833–849.
25. **Miskin, J. E., C. C. Abrams, L. C. Goatley, and L. K. Dixon.** 1998. A viral mechanism for inhibition of the cellular phosphatase calcineurin. Science **281:**562–565.
26. **Mocarski, J. E. S.** 2002. Immunomodulation by cytomegaloviruses: manipulative strategies beyond evasion. Trends Microbiol. **10:**332–339.
27. **Moffat, K., G. Howell, C. Knox, G. J. Belsham, P. Monaghan, M. D. Ryan, and T. Wileman.** 2005. Effects of foot-and-mouth disease virus nonstructural proteins on the structure and function of the early secretory pathway: 2BC but not 3A blocks endoplasmic reticulum-to-Golgi transport. J. Virol. **79:**4382–4395.
28. **Netherton, C., I. Rouiller, and T. Wileman.** 2004. The subcellular distribution of multigene family 110 proteins of African swine fever virus is determined by differences in C-terminal KDEL endoplasmic reticulum retention motifs. J. Virol. **78:**3710–3721.
29. **Powell, P. P., L. K. Dixon, and R. M. E. Parkhouse.** 1996. An IκB homolog encoded by African swine fever virus provides a novel mechanism for down-regulation of proinflammatory cytokine responses in host macrophages. J. Virol. **70:**8527–8533.
30. **Prados, F. J., E. Viñuela, and A. Alcamí.** 1993. Sequence and characterization of the major early phosphoprotein p32 of African swine fever virus. J. Virol. **67:**2475–2485.
31. **Presley, J. F., N. B. Cole, T. A. Schroer, K. Hirschberg, K. J. M. Zaal, and J. Lippincott-Schwartz.** 1997. ER-to-Golgi transport visualized in living cells. Nature **389:**81–85.
32. **Rijnboutt, S., W. Stoorvogel, H. J. Geuze, and G. J. Strous.** 1992. Identification of subcellular compartments involved in biosynthetic processing of cathepsin D. J. Biol. Chem. **267:**15665–15672.
33. **Rodríguez, J. M., R. J. Yáñez, F. Almazán, E. Viñuela, and J. F. Rodriguez.** 1993. African swine fever virus encodes a CD2 homolog responsible for the adhesion of erythrocytes to infected cells. J. Virol. **67:**5312–5320.
34. **Saraste, J., and E. Kuismanen.** 1984. Pre- and post-Golgi vacuoles operate in the transport of Semliki forest virus membrane glycoproteins to the cell surface. Cell **38:**535–549.

35. **Sun, H., S. C. Jacobs, G. L. Smith, L. K. Dixon, and R. M. E. Parkhouse.** 1995. African swine fever virus gene j13L encodes a 25-27kDa virion protein with variable numbers of amino acid repeats. J. Gen. Virol. **76:**1117–1127.
36. **Tait, S. W. G., E. B. Reid, D. R. Greaves, T. E. Wileman, and P. P. Powell.** 2000. Mechanism of inactivation of NF-κB by a viral homologue of IκBα. J. Biol. Chem. **275:**34656–34664.
37. **Tartakoff, A. M.** 1986. Temperature and energy dependence of secretory protein transport in the exocrine pancreas. EMBO J. **5:**1477–1482.
38. **Wilkinson, P. J.** 1989. African swine fever virus, p. 17–35. *In* M. B. Pensaert (ed.), Virus infections of porcines. Elsevier Science Publishers, Amsterdam, The Netherlands.
39. **Wisner, T. W., and D. C. Johnson.** 2004. Redistribution of cellular and herpes simplex virus proteins from the trans-Golgi network to cell junctions without enveloped capsids. J. Virol. **78:**11519–11535.
40. **Yáñez, R. J., J. M. Rodríguez, M. L. Nogal, L. Yuste, C. Enríquez, J. F. Rodríguez, and E. Viñuela.** 1995. Analysis of the complete nucleotide sequence of African swine fever virus. Virology **208:**259–278.
41. **Yang, W., and B. Storrie.** 1998. Scattered Golgi elements during microtubule disruption are initially enriched in *trans*-Golgi proteins. Mol. Biol. Cell **9:**191–207.
42. **Ying, M., S. Grimmer, T. G. Iversen, B. van Deurs, and K. Sandvig.** 2003. Cholesterol loading induces a block in the exit of VSVG from the TGN. Traffic **4:**772–784.